

ENERGY-EFFICIENT WALKING OVER IRREGULAR TERRAIN: A CASE OF HEXAPOD ROBOT

**Mindaugas Luneckas¹⁾, Tomas Luneckas¹⁾, Dainius Udris¹⁾, Darius Plonis¹⁾,
Rytis Maskeliunas^{2,3)}, Robertas Damasevicius³⁾**

1) Vilnius Gediminas Technical University, Faculty of Electronics, Naugarduko g. 41, 03227 Vilnius, Lithuania
(mindaugas.luneckas@vgtu.lt, tomas.luneckas@vgtu.lt, dainius.udris@vgtu.lt, darius.plonis@vgtu.lt)

2) Kaunas University of Technology, Department of Multimedia Engineering, K. Baršausko 59-A338, LT-51423, Kaunas,
Lithuania (rytis.maskeliunas@ktu.lt)

3) Silesian University of Technology, Faculty of Applied Mathematics, Kaszubska 23, 44-100 Gliwice, Poland
(robertas.damasevicius@polsl.pl, +370 37 300 353)

Abstract

Adaptive locomotion over difficult or irregular terrain is considered as a superiority feature of walking robots over wheeled or tracked machines. However, safe foot positioning, body posture and stability, correct leg trajectory, and efficient path planning are a necessity for legged robots to overcome a variety of possible terrains and obstacles. Without these properties, any walking machine becomes useless. Energy consumption is one of the major problems for robots with a large number of Degrees of Freedom (DoF). When considering a path plan or movement parameters such as speed, step length or step height, it is important to choose the most suitable variables to sustain long battery life and to reach the objective or complete the task successfully. We change the settings of a hexapod robot leg trajectory for overcoming small terrain irregularities by optimizing consumed energy and leg trajectory during each leg transfer. The trajectory settings are implemented as a part of hexapod robot simulation model and tested through series of experiments with various terrains of differing complexity and obstacles of various sizes. Our results show that the proposed energy-efficient trajectory transformation is an effective method for minimizing energy consumption and improving overall performance of a walking robot.

Keywords: hexapod walking robot, irregular terrain, obstacle avoidance, energy consumption, leg trajectory optimization.

© 2019 Polish Academy of Sciences. All rights reserved

1. Introduction

Research on walking robots has become more frequent as a research object due to their resemblance to animals or insects that have developed most effective methods for adaptive movement and energy efficiency through billions years of evolution. In nature, there are no animals that use wheels instead of legs to move [1], while multi-leg animals such as insects or

spiders can traverse rough terrains with high speed and in energy-efficient way. Legged robots with many *Degrees of Freedom* (DoF) excel the wheeled robots in movement flexibility and adaptability to different terrains by their ability to actively adjust the body height in order to ensure their stability and balance [2]. As a result, legged robots can overcome obstacles that are larger than the similarly sized wheeled robots and are limited only by the length of the robot's leg.

Adaptive locomotion and energy consumption are major challenges for all walking robots [3]. Specifically, hexapod walking robots have attracted considerable attention because of their stability due to always having at least three supporting legs. Also, they have high ability in walking in complex and unstructured environments such as industrial sites or disaster areas [4], variable geometry, manoeuvrability, omnidirectional movement, low footprint, high fault tolerance, faster walking speed and a large number of different gaits available [5]. Any modification of gait configurations results in numerous opportunities for optimization as well as research challenges [6]. Finally, robots with six or more legs do not usually require profound dynamic kinematics analysis, because of their static and dynamic stability.

Many robotic scientists have addressed problems of multi-legged walking over irregular terrain such as quadruped robot with a neural system model to implement online dynamic walking [7], generation of gait using *zero-moment point* (ZMP) condition and energy-feedback control [8], adaptive gait capable of generating reactive stepping for hexapod robot with sensor feedback [9] and fault-tolerant gait for adaptive locomotion [10]; *Central Pattern Generator* (CPG)-based locomotion methodology along with force feedback in order to generate adaptive gaits [1], bio-heuristic control strategy based on the CPG model using Hopf oscillators and *Radial Basis Function Neural Network* (RBFNN) [11]; a *fully connected Recurrent Neural Network* (FCRNN) with *multi-objective continuous ant colony optimization* (AMO-CACO) for gait generation of a biped robot [12]; using Bezier curves to optimize foot trajectory and improve the motion performance of a quadruped robot [13]; adaptive step size depending upon the identified terrain type [14] and adaptive walking controlled by a neuro-mechanical controller with *Modular Neural Network* (MNN) coupled with sensorimotor learning [15].

The problem of high energy consumption in walking robots comes from a large number of DoF. Most quadruped robots have 12–16 DoF while most hexapod robots have 18–24 DoF. This makes energy minimization a difficult task that requires in-depth analysis on how energy consumption depends on robot walking parameters (such as step length and height), gait styles, etc. Minimizing energy loss can be implemented by analysing and selecting best fitting gait style or gait parameters [16–21] or by observing turning motion [22]. However, in all these works only wave and tripod gaits were used and no other walking patterns were included.

Other works on minimization of energy consumption include the development of a more complete dynamics model [23], design of efficient actuators [24, 25], extending the bearing fatigue life for leg joints [26], development of elastic load suspension mechanism [27], new leg design [28], or a control system with *genetic algorithm* (GA) to observe battery life and move to recharge station location [29], a dynamical model considering the inertial effects of the legs [30], and GA combined with inverse kinematics and trajectory planning [4]. None of these papers studied a more important aspect of walking robots, which is their ability to overcome obstacles. Being able to minimize energy consumption while robot is traversing over various terrains would make walking robots more reliable in real missions. Recently, there have been some attempts to develop methods for walking over irregular terrain and minimizing energy consumption. Still, most of these works did not consider the complexity of terrain.

In our previous work, we have analysed energy consumption of a hexapod robot walking in an obstacle-free terrain [31]. Here, we address the problem of minimizing energy consumption of a

hexapod robot while moving over a terrain with small-sized obstacles. The robot leg trajectory is constructed to overcome obstacles and different trajectories are generated by changing step height and width. Average energy consumption is calculated to evaluate efficiency of the method.

The remaining parts of the paper are organized as follows. We provide a formal description of terrain, a method for calculating energy consumption, and leg trajectory optimization in Section 2. The experiments, the obtained results and their analysis are presented in Section 3. Finally, we present conclusions in Section 4.

2. Methods

2.1. Robot model and constraints

We use an Hexa V4 walking robot with the hexagon type body shape (Fig. 1). Hexa V4 is a small robot, its mass is 1.5 kg; mass of each leg is 0.2 kg. Each leg has 3 servo motors AX-12, making HexaV4 an 18-DoF machine. Servo motors AX-12 use 900 mA maximum input current, while STM32 microcontroller consumes only 100 μ A/MHz. The control system is combined from STM32F411RE, a data direction converter (74HC126 and 74HC04), and a voltage converter 7805 which is used to convert input voltage to 5 V, because the microcontroller uses 5 V voltage, while servo motors require 10–12 V input to fully function. We also use a 16 MHz external oscillator, which needs around 1.6 mA during run time. This is almost 6 times less than current consumption of one servo motor. To monitor the current consumption, we use an INA169 current sensor. The legs of HexaV4 are constructed from three parts: coxa, femur, and tibia (Fig. 3), which have the following dimensions: 5 cm, 8.5 cm, and 12 cm, respectively. In neutral stance, all tibia leg parts are positioned at 90° and the robot body is elevated at 10 cm. This is the standard position for neutral movement for this robot. The step length, height, and width depend on the femur part of leg. In theory, the largest step length, height, and width of Hexa V4 robot are $l_{\max} = h_{\max} = w_{\max} = 10$ cm. However, due to the mechanical constraints, the step width can reach only up to 6 cm.

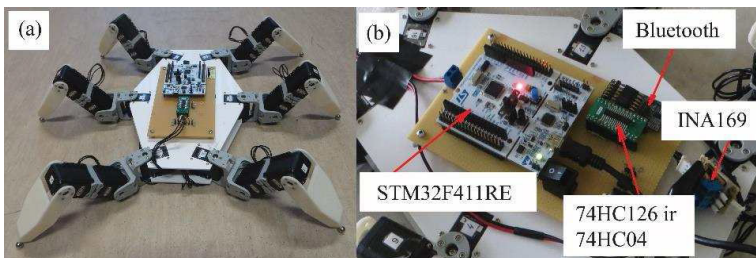


Fig. 1. A hexapod robot HexaV4 with main components.

2.2. Formal description of terrain

Terrain classification is based on the characteristics of a specific robot such as its step length, height, and width, which are defined by the robot dimensions. Each obstacle can be described by three dimensions: length L , height H , and width W (Fig. 2). We limit the problem of energy-efficient walking over irregular terrain to only small obstacles along the straight path, and introduce two types of terrain:

- Flat surface. The irregularities are so small that they can be ignored and changing the robot movement path is not necessary. Obstacles are characterized as follows:

$$\{L < l_i; H < h_i; W < w_i\}, \tag{1}$$

where l_i, h_i, w_i – a robot’s initial step length, height, and width, respectively. A step length is measured in the direction of the forward/backward motion of a robot. A step height is measured in the direction of the upwards/downward motion of a robot. A step width is measured in the direction of the left/right motion of a robot.

- Blocking terrain irregularities. These obstacles cannot be overcome with initial parameters and require changing the leg trajectory. Small obstacles are characterized as follows:

$$\begin{cases} l_i < L < l_{\max} \\ h_i < H < h_{\max} \\ w_i < W < w_{\max} \end{cases}, \tag{2}$$

where $l_{\max}, h_{\max}, w_{\max}$ – a robot’s maximum step length, height, and width, respectively.

We assume that a robot already has information about its walking path and all dimensions of upcoming irregularities such as obstacles that block the path for a robot are also known (Fig. 2). A robot’s traverse of an obstacle is dependent only on a robot’s step height, length and width. Other obstacles that not affect the robot’s movement (since they either stay far from the robot or go below the robot body) are not considered; therefore, the robot’s walking controller has to process less information when compared with the vision-based systems, where a full world map is usually generated.

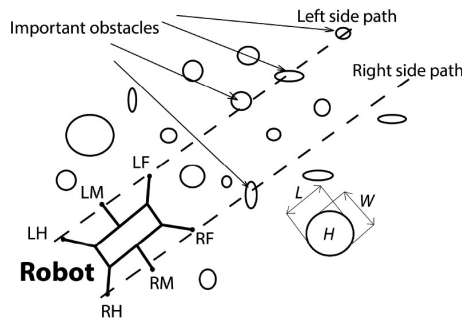


Fig. 2. Terrain irregularities blocking the left and right sides of the robot. The left side is the path of the *left hind* (LH); *left middle* (LM) and *left front* (LF) legs; the right side is the path of the *right hind* (RH); *right middle* (RM) and *right front* (RF) legs. L, H, and W are dimensions of an obstacle (length, height, width).

Basic hexapod gaits (tripod, tetrapod, ripple, and wave) differ by the sequence of leg transfer and swing/support phase time ratio. The step length of the robot must be larger than the length of an obstacle. If we change the step length, the gait synchronization will be lost, which will result in a jerky motion of servo motors. Therefore, the step length is only changed for a different speed of robot movement. Some obstacles may be higher and less wide making it easier to step around it. Other obstacles may be very wide, but not as high, which makes it easier for the robot to step above the obstacle (see Fig. 3). In any case, the robot should be able to change its leg trajectory according to the size of terrain irregularities in front of it.

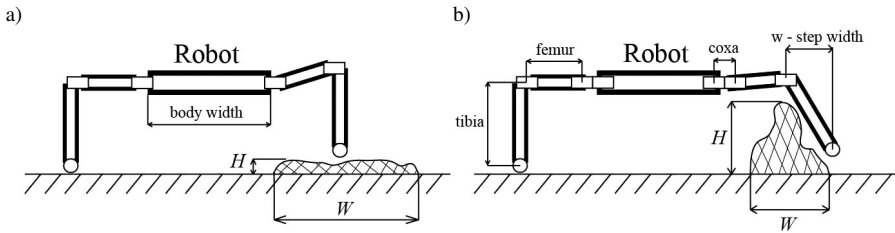


Fig. 3. Different ways of overcoming various terrain irregularities: going above the obstacle (left) and going around the obstacle (right).

2.3. Optimization of leg trajectory

The leg trajectory of a hexapod robot is composed of the linear part and the sinusoidal arc. The leg trajectory coordinates can be calculated as follows:

$$x_{fi}(t) = \begin{cases} -\cos(\varepsilon) \cdot \left(\frac{l \cdot (T - 2 \cdot \varphi_i + 2 \cdot t - 1)}{2 \cdot (T - 1)} + \frac{l}{2} \right), & \text{if } t \leq \varphi_i, \\ \cos(\varepsilon) \cdot l \cdot (T - \varphi_i), & \text{if } \varphi_i < t \leq \varphi_i + 1; \\ \cos(\varepsilon) \cdot \left(\frac{l \cdot (T + 2 \cdot \varphi_i - 2 \cdot t + 1)}{2 \cdot (T - 1)} + \frac{l}{2} \right), & \text{if } t > \varphi_i + 1, \end{cases} \quad (3)$$

$$y_{fi}(t) = \begin{cases} -\sin(\varepsilon) \cdot \left(\frac{l \cdot (T - 2 \cdot \varphi_i + 2 \cdot t - 1)}{2 \cdot (T - 1)} + \frac{l}{2} \right), & \text{if } t \leq \varphi_i, \\ \sin(\varepsilon) \cdot (l \cdot (t - \varphi_i)), & \text{if } \varphi_i < t \leq \varphi_i + 1; \\ \sin(\varepsilon) \cdot \left(\frac{l \cdot (T + 2 \cdot \varphi_i - 2 \cdot t + 1)}{2 \cdot (T - 1)} + \frac{l}{2} \right), & \text{if } t > \varphi_i + 1, \end{cases} \quad (4)$$

$$z_{fi}(t) = \begin{cases} 0, & \text{if } t \leq \varphi_i; \\ h \cdot \sin((t - \varphi_i) \cdot \pi), & \text{if } \varphi_i < t \leq \varphi_i + 1, \\ 0, & \text{if } t > \varphi_i + 1; \end{cases} \quad (5)$$

where: h – step height; T – gait period; t – time; φ – phase; ε – angle of movement direction.

A leg phase φ is expressed as points in time, when certain changes in the leg trajectory happen (for example, when the leg either starts moving up or touches the surface). This parameter is dependent on the gait type. Each leg has a unique phase depending on the gait type, which shows the time that the exact leg has to be either in the support or transfer phase. A gait period T is also a unit of time showing the duration of a specific gait. A gait period always has a value of 2 or more, because otherwise the robot would not be able to move.

To modify the leg trajectory, we add the leg motion in zy plane to the trajectory and change $y(t)$ coordinate as follows:

$$y_{fi}(t) = \begin{cases} -\sin(\varepsilon) \cdot \left(\frac{l \cdot (T - 2 \cdot \varphi_i + 2 \cdot t - 1)}{2 \cdot (T - 1)} + \frac{l}{2} \right), & \text{if } t \leq \varphi_i, \\ \sin(\varepsilon) \cdot (l \cdot (t - \varphi_i)) + w \cdot \sin((t - \varphi_i) \cdot \pi), & \text{if } \varphi_i < t \leq \varphi_i + 1, \\ \sin(\varepsilon) \cdot \left(\frac{l \cdot (T + 2 \cdot \varphi_i - 2 \cdot t + 1)}{2 \cdot (T - 1)} + \frac{l}{2} \right), & \text{if } t > \varphi_i + 1, \end{cases} \quad (6)$$

where w – step width.

Equations (3), (4), and (6) form the required obstacle-avoiding leg trajectory. The leg trajectory distance d consists of two parts: the linear and sinusoidal arc ones:

$$d_{leg} = l + s, \tag{7}$$

where l is the robot's step length, and s is the sinusoidal arc length, which has the form:

$$s = \int_a^b \sqrt{[dx(t)/dt]^2 + [dy(t)/dt]^2 + [dz(t)/dt]^2} dt. \tag{8}$$

The leg trajectory is half the sinusoidal arc, which means that integration must be done from 0 to π . Also, the sine arc applies only to $y(t)$ and $z(t)$ coordinates, because $x(t)$ coordinate represents the step length. Having this in mind, we can combine (9), (10) and derive the final form of the sinusoidal arc as follows:

$$s = \int_0^\pi \sqrt{\frac{4 + \pi^2 \cdot w^2 \cdot \cos^2((\varphi_i - t) \cdot \pi/2) + \pi^2 \cdot h^2 \cdot \cos^2((\varphi_i - t) \cdot \pi/2)}{4}} dt. \tag{9}$$

2.4. Calculation of energy consumption

Energy consumption is calculated as follows:

$$E = \int_0^T P(t) dt = \int_0^T U(t) \cdot I(t) dt, \tag{10}$$

where: $P(t)$ – instantaneous power; $U(t)$ – voltage; $I(t)$ – current; and T – operation time of the robot.

Voltage is defined by the *electromotive function* (EMF):

$$U(t) = R \cdot I(t) + L \frac{dI(t)}{dt} + k_E \theta'' \tag{11}$$

where: R – electric resistance of the motor; L – rotor inductance; k_E – EMF constant and $\dot{\theta}_m$ – speed of the motor.

We can ignore power consumption of the robot microcontroller as it does not have a substantial influence on overall power consumption. Having this in mind, we only need to calculate the energy consumption of the robot's legs. However, (10) is not completely suitable because the operation time of each separate leg is not known. Instead, we know the speed and leg trajectory distance of the robot's legs. We can calculate the energy consumed by an individual leg in a single trajectory as follows:

$$E_{leg} = U(t) \cdot I_{leg}(t) \cdot \frac{d_{leg}}{v}, \tag{12}$$

where: d_{leg} – trajectory distance of a single robot leg; v – leg movement speed; I_{leg} – leg current consumption. The leg movement acceleration is not considered, even though the legs are constantly accelerating and decelerating (*i.e.*, have a sinusoidal profile). However, we are measuring the current energy consumption of each of the robot's legs, which depends on the leg movement acceleration and the leg speed.

Finally, we can express the energy consumption of the robot as follows:

$$E = \sum_{leg=1}^N E_{leg}, \quad (13)$$

where N the number of robot legs.

To find the shortest and most energy-effective robot trajectory overcoming the terrain obstacles, optimization is needed. As energy consumption depends on the leg trajectory distance and current consumption, the optimization problem can be solved for the minimum leg trajectory distance and the minimum energy consumption as follows:

$$\arg \min_{I_{leg}=f(w,h)} (E_{leg}), \quad \text{subject to } w \in [0 \text{ cm}, 6 \text{ cm}], \quad h \in [0 \text{ cm}, 10 \text{ cm}], \quad I_{leg} = f(w, h). \quad (14)$$

The evaluation of energy-efficient leg trajectory is performed in two steps. First, the energy consumption is calculated without trajectory optimization, when the robot moves its legs over the obstacles. For this case, the step parameters are: $w = 0$; $h = H$. Next, the leg trajectory is transformed to go around the obstacle, and the energy consumption is calculated with step parameters: $w = W$; $h = h_i$. Note that the step height is set to the initial height value. This parameter value remains unchanged because if the obstacle size satisfies the constraints then the robot will not change its body elevation to overcome the obstacle without collision (the body elevation is set to 10 cm).

2.5. Kinematics model of hexapod robot

In order to obtain close-to-real-world simulation of robot kinematics, gaits, leg trajectory, energy optimization, and robot locomotion over irregular terrain, we have developed a kinematics model of a hexapod robot in MATLAB (Version R2016b, MathWorks, Natick, MA, USA). The kinematics model of a robot is shown in Fig. 4.

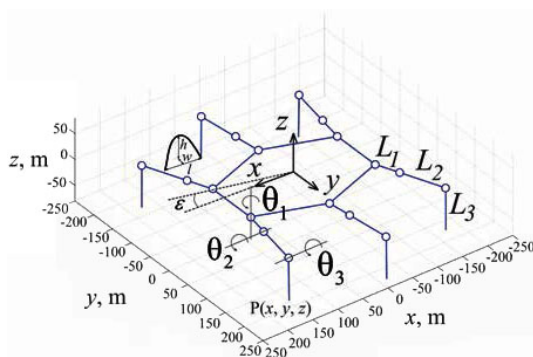


Fig. 4. The kinematics model of a hexapod robot in MATLAB: L_1 – length of coxa; L_2 – length of femur and L_3 – length of tibia; θ_1 – angle of coxa, θ_2 – angle of femur, θ_3 – angle of tibia (adopted from [32]).

2.6. Measurement of current consumption

To measure the current consumption of a physical hexapod robot, we use an INA169 high-speed current shunt monitor, which is connected directly to an oscilloscope (Fig. 5). The average

current I_{avg} is obtained from the current measurements as follows:

$$I_{avg} = \frac{I_1 + I_2 + \dots + I_n}{n}, \quad (15)$$

where n – the number of points.

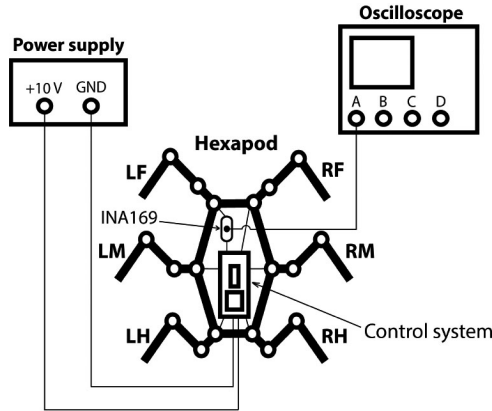


Fig. 5. A diagram of current consumption measurement. The current shunt monitor INA169 is connected between the power supply and the left front (LF) robot leg.

3. Experimental settings and results

3.1. Terrain and obstacles

In practice, we use two types of obstacles: small ($3 \text{ cm} \leq H \leq 5 \text{ cm}$), and large ($6 \text{ cm} \leq H \leq 8 \text{ cm}$). During the experiments we did not use obstacles with heights between 5 and 6 cm. However, in case they would appear along the robot's path, they would be treated as large obstacles. Examples of obstacles and their comparison with a hexapod robot are presented in Fig. 6.

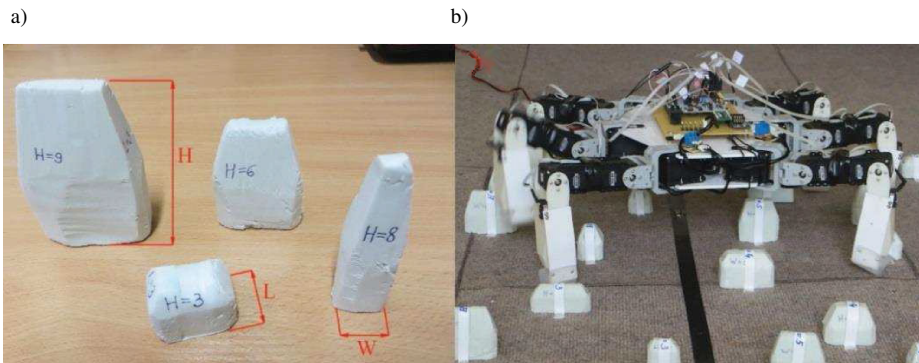


Fig. 6. Examples of real obstacles: a) obstacle parameters; b) comparison of obstacle sizes with a hexapod robot.

3.2. Robot simulation

During the robot simulation in MATLAB, we used three types of terrain of different obstacle densities: low-density (10 obstacles over a given distance), medium-density (20 obstacles) and high-density (30 obstacles) terrain (Fig. 7). All obstacles in the model were described by parameters such as length, width, height, and x and y coordinates, which outlined the position of each obstacle in the environment and were used to simulate the avoidance of obstacles in the robot. The speed of each leg was set to the same value as the speed of the robot, thus ensuring that the movements of the legs are not synchronized in time (the leg speed becomes the same during the support and transfer phases). The initial movement parameters were as follows: step length $l = 4$ cm, height $h = 1$ cm. In all experiments, the robot walked over 3.2 m distance and overcome all obstacles. Since the robot and all the legs had to move at a constant speed all the time, no specific gait was selected for the tests. This means that only a single leg at a time would go into the transfer phase while other legs would be in the support phase. Thus, only one leg at a time would avoid the obstacle. Energy calculations were done separately by inserting necessary constant parameter values. The obstacle sizes were chosen randomly in order to simulate a real terrain.

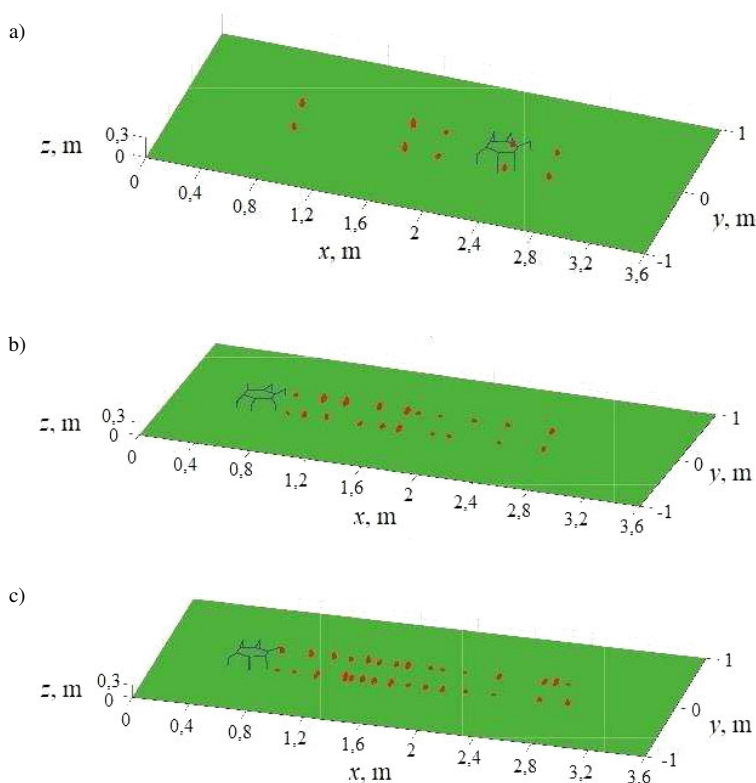


Fig. 7. Simulation examples of hexapod robot locomotion over different obstacle density terrains: a) low-density; b) average-density; c) high-density ones (adopted from [32]).

An example of the simulated trajectory according to (3), (4), (6) is presented in Fig. 8.

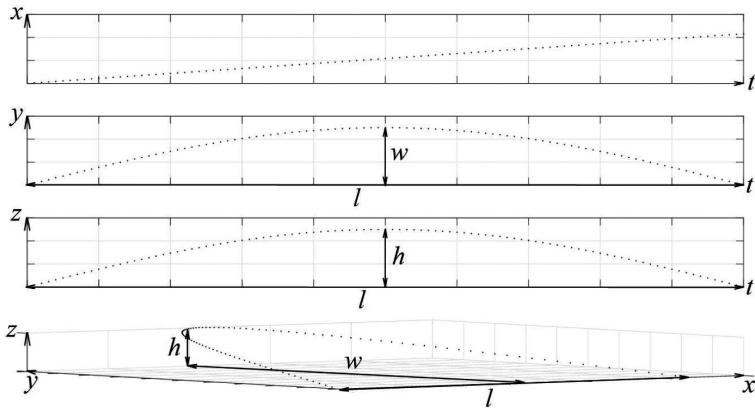


Fig. 8. An example of obstacle avoidance trajectory of a leg. From top to bottom: $x(t)$, $y(t)$, $z(t)$, and all coordinates combined together in 3D space.

3.3. Real-world experiments with physical hexapod robot

For real-world experiments with an Hexa V4 walking robot, three terrains of different complexity were used: low-complexity, average-complexity, and high-complexity ones. Each type of terrain differs by the number of obstacles along the robot path: a low-complexity terrain has 10 obstacles; an average-complexity terrain – 20 obstacles; and a high-complexity terrain – 30 obstacles (Fig. 9). The tripod gait was used through all experiments. The speed of robot movement was set the same as during the current consumption experiments, which is $v = 0.025$ m/s. The speed of robot leg movement was set to be equal to the speed of robot movement. The leg movement speed remained unchanged for both support and transfer phases. The initial parameters were set to: $l = 4$ cm, $h = 1$ cm. During each experiment run, the robot had to move over 3.2 m distance and overcome the same number of obstacles by each side of the robot (*i.e.*, 5, 10, and 15) depending on the terrain complexity. For all types of terrain, five runs were carried out with different sizes of obstacles.

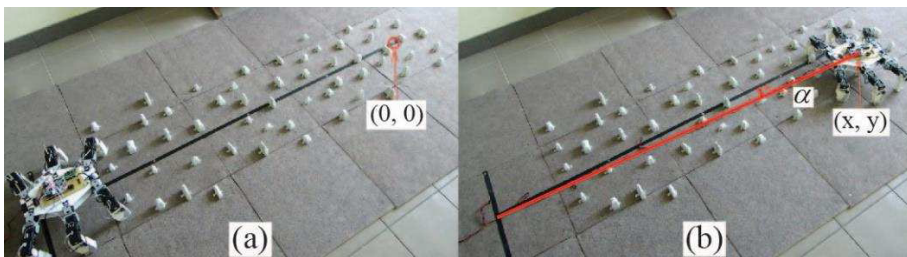


Fig. 9. Hexapod robot locomotion over a high-density terrain with small height obstacles using the wave gait: a) the robot position at the starting point; b) the robot position at the goal (adopted from [32]).

3.4. Results of current measurements

To evaluate the energy consumption, the measurements of the current consumption with respect to step height and step width were performed with a real hexapod robot HexaV4 using an INA169 high-speed current shunt monitor, which was connected directly to an oscilloscope

(Fig. 4). For all experiments, the robot movement speed was set to $v = 0.025$ m/s. The current consumption was measured for a single leg making several steps. Each combination (of step height and step width) was measured once giving 6000 current values.

The measurement results are presented in Table 1 and for better understandability summarized as a contour plot in Fig. 10. The values between the measurement points in the contour plot were interpolated using the cubic interpolation.

Table 1. Dependence of current consumption upon step height and step width of the robot.

	h (cm)									
	1	2	3	4	5	6	7	8	9	10
w (cm)	I_{avg} (A)									
0	0.194	0.202	0.205	0.208	0.208	0.207	0.219	0.219	0.218	0.224
1	0.197	0.203	0.204	0.209	0.207	0.215	0.214	0.216	0.221	0.222
2	0.258	0.202	0.205	0.206	0.210	0.208	0.211	0.217	0.219	0.219
3	0.256	0.245	0.198	0.203	0.206	0.205	0.213	0.212	0.212	0.214
4	0.215	0.244	0.236	0.205	0.208	0.204	0.206	0.208	0.211	0.213
5	0.252	0.248	0.230	0.215	0.201	0.207	0.209	0.209	0.209	0.211
6	0.252	0.254	0.247	0.234	0.223	0.208	0.203	0.209	0.208	0.208

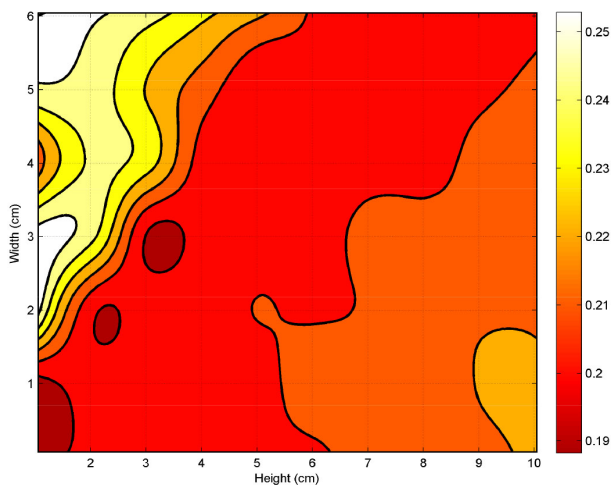


Fig. 10. A profile of current consumption as a function of robot step width and height.

3.5. Statistical analysis of measurement data

We performed the statistical analysis of the results using the Nemenyi post hoc test, which reports the significant differences between individual models after the Friedman test has rejected the null hypothesis that the performance of the comparisons on the groups of data is similar. The Friedman test assigns ranks to all models according to their performance. The average rank is given to the models if they have shown the same performance. The null hypothesis states that there is no difference between configurations that can be rejected or accepted according

to the value of Friedman test statistic. Fig. 11 shows the Demšar significance diagram [33], in which robot leg configurations are arranged on x axis as per their average rank and their corresponding ranks are given on y axis. The Demšar diagram displays the ranked performances of the compared configurations, along with the CD, to highlight any configurations which are significantly different. According to this test, two configurations are significantly different if their average rank differs by more than the *critical difference* (CD), which is calculated as follows:

$$CD = q\sqrt{\frac{K(K+1)}{D}}, \tag{16}$$

where: D – the number of datasets; K – the number of configurations and q is calculated on the basis of studentized range statistic. The results (Fig. 10) show that the statistically significant smallest energy consumption is provided by the $w = 0$ cm, $h = 1$ cm configuration.

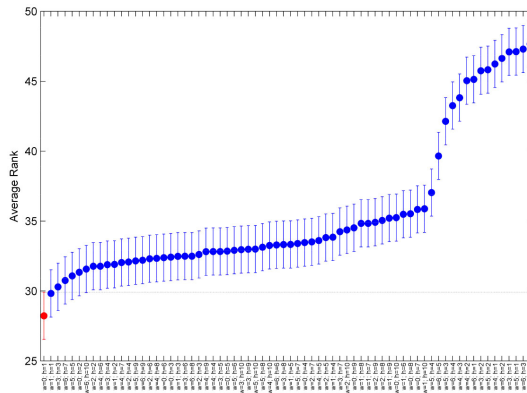


Fig. 11. Comparison of robot leg configurations: results of Nemenyi test.

Using the data from Table 1, the prediction model was obtained via multiple regression analysis as follows:

$$I = 0.01w - 0.0057h + 0.00079h^2 - 0.0015w \cdot h + 0.21, \tag{17}$$

where: I – current; w – width and h – height of the step. The significance levels of coefficients for the statistical prediction model 17 were all exceeding $p < 0.001$, while for the coefficient of h , the significance level exceeded $p < 0.01$. The *Root Mean Square Error* (RMSE) of the regression model is 0.0093, while $R^2 = 0.6348$ (adjusted $R^2 = 0.6123$).

3.6. Comparison of trajectory setting optimization results

The average energy consumption results obtained by simulation without and with optimization of robot walking trajectory settings for energy efficiency are presented in Fig. 12. The energy savings when using optimization of trajectory settings for energy efficiency are summarized in Fig. 13. The results show that the average efficiency of optimization of leg trajectory settings is 15% for a low-complexity terrain, 19.2% for an average-complexity terrain, and 18.4% for a high-complexity terrain, which means that the use of optimization of trajectory settings enables to decrease the energy consumption for different types of terrain.

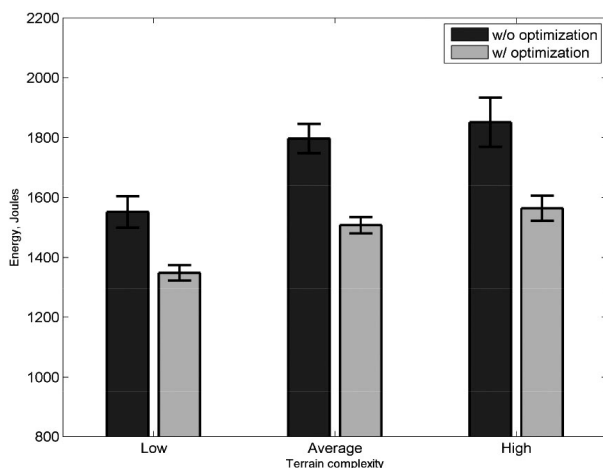


Fig. 12. Energy consumption of HexaV4 robot for terrains of different complexity.

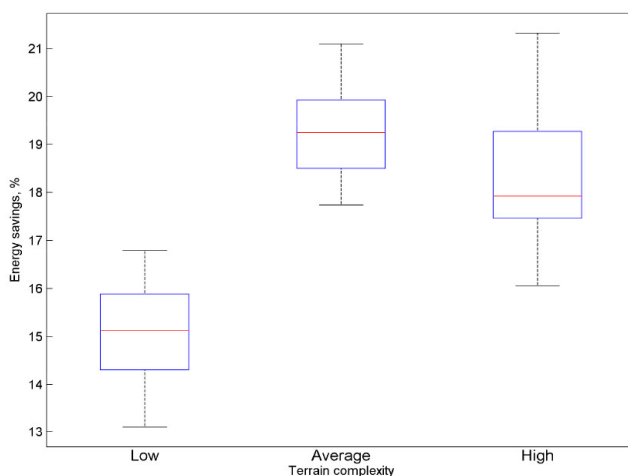


Fig. 13. Energy savings obtained with optimization of robot walking trajectory settings for energy efficiency.

We have performed the statistical analysis of the results using the non-parametric Wilcoxon rank-sum test and bootstrapping ($N = 10000$) test. The results show that the difference in energy savings is significant between low- and average- ($p < 0.001$), and low- and high-complexity ($p < 0.05$) terrains, respectively, but it is not significant between average- and high-complexity terrains. The differences between energy consumption of robot walking without and with optimization are significant for all types of terrain ($p < 0.001$).

Our results are in line with the efforts of other authors. For example, Zhang *et al.* [34] proposed a periodic gait optimization method based on energy consumption index and achieved a 14% reduction in energy consumption for a multi-legged robot. Chun *et al.* [35] achieved an improvement of 14.2% in energy consumption of an agricultural hexapod robot walking on a compacted soil ground in hilly areas using an optimization of joint positions.

4. Conclusion

We have analysed optimization of the robot leg trajectory transformation for the energy-efficient locomotion of a walking robot over an irregular terrain. We described optimization of a 3-DoF hexapod robot leg to minimize the leg trajectory distance and energy consumption. We used an HexaV4 robot for specification of constraints and MATLAB for simulation of terrains of different complexity. The simulation experiments were carried out for three different types of terrain complexity, each varying by the number of obstacles blocking the path of the robot. The current measurement results obtained from real-world experiments show efficiency of the proposed robot trajectory optimization method, which enabled to achieve a decrease in average robot energy consumption of over 17%. The proposed method can be used for any type of walking machine with any number of DoF of each leg.

References

- [1] Chen, W.H., Ren, G.J., Wang, J.H., Liu, D. (2014). An adaptive locomotion controller for a hexapod robot: Cpg, kinematics and force feedback. *Science China Information Science.*, 57(11), 1–18.
- [2] Li, R., Meng, H., Bai, S., Yao, Y., Zhang, J. (2018). Stability and gait planning of 3-UPU hexapod walking robot. *Robotics*, 7(3), 48.
- [3] Tedeschi, F., Carbone, G. (2014). Design issues for hexapod walking robots. *Robotics.*, 3(2), 181–206.
- [4] Zhu, Y., Jin, B., Li, W., Li, S. (2014). Optimal design of hexapod walking robot leg structure based on energy consumption and workspace. *Transactions of the Canadian Society for Mechanical Engineering*, 38(3), 305–317.
- [5] Wang, Z.Y., Ding, X.L., Rovetta, A. (2009). Analysis of typical locomotion of a symmetric hexapod robot. *Robotica*, 28(06), 893–907.
- [6] Sheba, J.K., Elara, M., Martinez-Garcia, E., Le, T.P. (2016). Trajectory generation and stability analysis for reconfigurable klann mechanism based walking robot. *Robotics*, 5(3), 13.
- [7] Kimura, H., Fukuoka, Y., Cohen A.H. (2007). Adaptive dynamic walking of a quadruped robot on natural ground based on biological concepts. *The International Journal of Robotics Research*, 26(5), 475–490.
- [8] Asano, F., Yamakita, M., Kamamichi, N., Luo, Z.W. (2004). A novel gait generation for biped walking robots based on mechanical energy constraint. *IEEE Transactions on Robotics and Automation*, 20(3), 565–573.
- [9] Asif, U., Iqbal, J. (2011). An approach to stable walking over uneven terrain using a reflex-based adaptive gait. *Journal of Control Science and Engineering*, 16.
- [10] Asif, U. (2012). Improving the navigability of a hexapod robot using a fault-tolerant adaptive gait. *International Journal of Advanced Robotic Systems*, 9(2), 34.
- [11] Zeng, Y., Li, J., Yang, S., Ren, E. (2018). A bio-inspired control strategy for locomotion of a quadruped robot. *Applied Sciences*, 8(1), 56.
- [12] Juang, C.F., Yeh, Y.T. (2018). Multiobjective evolution of biped robot gaits using advanced continuous ant-colony optimized recurrent neural networks. *IEEE Transactions on Cybernetics*, 48(6), 1910–1922.
- [13] Meng, G., Ya-nan, L., Qing-sheng, L., Ning, S. (2017). Optimization and simulation on key parameters of foot trajectory for a hydraulic quadruped robot. *IEEE International Conference on Robotics and Biomimetics, ROBIO, Macau*, 1454–1459.

- [14] Walas, K., Kanoulas, D., Kryczka, P. (2016). Terrain classification and locomotion parameters adaptation for humanoid robots using force/torque sensing. *2016 IEEE-RAS 16th International Conference on Humanoid Robots (Humanoids)*, 133–140.
- [15] Xiong, X., Wörgötter, F., Manoonpong, P. (2016). Adaptive and energy efficient walking in a hexapod robot under neuromechanical control and sensorimotor learning. *IEEE Transactions on Cybernetics*, 46(11), 2521–2534.
- [16] Kar, D.C., Kurien, I.K., Jayarajan, K. (2001). Minimum energy force distribution for a walking robot. *Journal of Field Robotics*, 18(2), 47–54.
- [17] Roy, S.S., Pratihari, D.K. (2011). Dynamic modeling and energy consumption analysis of crab walking of a six-legged robot. *2011 IEEE Conference on Technologies for Practical Robot Applications (TePRA)*, 82–87.
- [18] Kottege, N., Parkinson, C., Moghadam, P., Elfes, A., Singh, S.P.N. (2015). Energetics-informed hexapod gait transitions across terrains. *2015 IEEE International Conference on Robotics and Automation (ICRA)*, 5140–5147.
- [19] Mahapatra, A., Roy, S.S., Bhavanibhatla, K., Pratihari, D.K. (2015). Energy-efficient inverse dynamic model of a hexapod robot. *2015 International Conference on Robotics, Automation, Control and Embedded Systems (RACE)*, 1–7.
- [20] Zielinska, T. (2015). Walking machines for exploration-optimizing the energy spendings. *2015 10th International Workshop on Robot Motion and Control (RoMoCo)*, 124–129.
- [21] Gonzalez de Santos, P., Garcia, E., Ponticelli, R., *et al.* (2009). Minimizing energy consumption in hexapod robots. *Advanced Robotics*, 23(6), 681–704.
- [22] Roy, S.S., Pratihari, D.K. (2014). Kinematics, dynamics and power consumption analyses for turning motion of a six-legged robot. *Journal of Intelligent & Robotic Systems*, 74(3–4), 663.
- [23] Lin, B.S., Song, S.M. (2001). Dynamic modeling, stability, and energy efficiency of a quadrupedal walking machine. *Journal of Field Robotics*, 18(11), 657–670.
- [24] Estremera, J., Waldron, K.J. (2008). Thrust control, stabilization and energetics of a quadruped running robot. *The International Journal of Robotics Research*, 27(10), 1135–1151.
- [25] Vanderborght, B., Van Ham, R., Lefeber, D., *et al.* (2009). Comparison of mechanical design and energy consumption of adaptable, passive-compliant actuators. *The International Journal of Robotics Research*, 28(1), 90–103.
- [26] Wu, X., Li, Y., Consi, T.R. (2010). Life extending minimum-time path planning for a hexapod robot. In: *ASME 2010 Dynamic Systems and Control Conference; American Society of Mechanical Engineers*, 809–816.
- [27] Ackerman, J., Seipel, J. (2013). Energy efficiency of legged robot locomotion with elastically suspended loads. *IEEE Transactions on Robotics*, 29(2), 321–330.
- [28] Gonzalez-Rodriguez, A.G., Gonzalez-Rodriguez, A., Castillo-Garcia, F. (2014). Improving the energy efficiency and speed of walking robots. *Mechatronics*, 24(5), 476–488.
- [29] Parker, G., Zbeda, R. (2014). Learning area coverage for a self-sufficient hexapod robot using a cyclic genetic algorithm. *IEEE Systems Journal*, 8(3), 778–790.
- [30] Mahapatra, A., Roy, S.S., Pratihari, D.K. (2019). Study on feet forces' distributions, energy consumption and dynamic stability measure of hexapod robot during crab walking. *Applied Mathematical Modelling*, 65, 717–744.
- [31] Luneckas, M., Luneckas, T., Udriš, D., *et al.* (2014). Hexapod robot energy consumption dependence on body elevation and step height. *Elektronika ir Elektrotechnika*, 20(7), 7–10.

- [32] Luneckas, L. (2018). *Investigation of Energy Efficiency of Hexapod Robot Locomotion Doctoral Dissertation*. Vilnius Gediminas Technical University.
- [33] Demsar, J. (2006). Statistical comparisons of classifiers over multiple data sets. *Journal of Machine Learning Research*, 7, 1–30.
- [34] Zhang, S., Xing, Y., Hu, Y. (2018). Composite gait optimization method for a multi-legged robot based on optimal energy consumption. *Journal of Chinese Space Science and Technology*.
- [35] Chun, Z., Mingjin, Y., Jian, C., et al. (2016). Energy consumption optimization model of agricultural hexapod robot with self-locking joints. *Transactions of the Chinese Society of Agricultural Engineering*, 32(18), 73–83.